

AD_____

Award Number: W81XWH-04-1-0170

TITLE: Inhibitors of Histone Deacetylases for Radiosensitization
of Prostate Cancer

PRINCIPAL INVESTIGATOR: Mira O. Jung, Ph.D.

CONTRACTING ORGANIZATION: Georgetown University Medical Center
Washington, DC 20007

REPORT DATE: February 2005

TYPE OF REPORT: Annual

PREPARED FOR: U.S. Army Medical Research and Materiel Command
Fort Detrick, Maryland 21702-5012

DISTRIBUTION STATEMENT: Approved for Public Release;
Distribution Unlimited

The views, opinions and/or findings contained in this report are those of the author(s) and should not be construed as an official Department of the Army position, policy or decision unless so designated by other documentation.

20050603 167

REPORT DOCUMENTATION PAGEForm Approved
OMB No. 074-0188

Public reporting burden for this collection of information is estimated to average 1 hour per response, including the time for reviewing instructions, searching existing data sources, gathering and maintaining the data needed, and completing and reviewing this collection of information. Send comments regarding this burden estimate or any other aspect of this collection of information, including suggestions for reducing this burden to Washington Headquarters Services, Directorate for Information Operations and Reports, 1215 Jefferson Davis Highway, Suite 1204, Arlington, VA 22202-4302, and to the Office of Management and Budget, Paperwork Reduction Project (0704-0188), Washington, DC 20503

1. AGENCY USE ONLY

(Leave blank)

2. REPORT DATE

February 2005

3. REPORT TYPE AND DATES COVERED

Annual (12 Jan 2004 - 11 Jan 2005)

4. TITLE AND SUBTITLEInhibitors of Histone Deacetylases for Radiosensitization
of Prostate Cancer**5. FUNDING NUMBERS**

W81XWH-04-1-0170

6. AUTHOR(S)

Mira O. Jung, Ph.D.

7. PERFORMING ORGANIZATION NAME(S) AND ADDRESS(ES)Georgetown University Medical Center
Washington, DC 20007

E-Mail: jungm@georgetown.edu

**8. PERFORMING ORGANIZATION
REPORT NUMBER****9. SPONSORING / MONITORING****AGENCY NAME(S) AND ADDRESS(ES)**U.S. Army Medical Research and Materiel Command
Fort Detrick, Maryland 21702-5012**10. SPONSORING / MONITORING
AGENCY REPORT NUMBER****11. SUPPLEMENTARY NOTES****12a. DISTRIBUTION / AVAILABILITY STATEMENT**

Approved for Public Release; Distribution Unlimited

12b. DISTRIBUTION CODE**13. ABSTRACT (Maximum 200 Words)**

Failure of conventional treatment of prostate cancer with radiotherapy may be due to intrinsic resistance of the tumor cells. One of mechanisms underlying intrinsic radiation sensitivity is linked to the state of chromatin architecture. The long-term goal of this proposal is to develop a novel therapeutic strategy by enhancing radiosensitivity of prostate cancer cells by testing the hypothesis that an increase of cellular radiation sensitivity may be achieved by exposure of cells to specific HDAC inhibitors. During the first year of the research funding period, the major accomplishment and significance of the research include: (1) determination of the values of 50% HDAC inhibition activities of newly synthesized HDAC inhibitors and their anti-proliferation activities. (2) Determination of efficacy of HDAC inhibitors on cellular radiation sensitivity.

14. SUBJECT TERMS

Radiation sensitivity, histone deacetylase, cytotoxicity

15. NUMBER OF PAGES

13

16. PRICE CODE**17. SECURITY CLASSIFICATION
OF REPORT**

Unclassified

**18. SECURITY CLASSIFICATION
OF THIS PAGE**

Unclassified

**19. SECURITY CLASSIFICATION
OF ABSTRACT**

Unclassified

20. LIMITATION OF ABSTRACT

Unlimited

INTRODUCTION

Key nuclear processes, including transcription, DNA replication, cell cycle and damage repair are affected by chromatin structure modification through the actions of histone acetyltransferases (HATs) and histone deacetylases (HDACs). Moreover, inhibition of HDACs shifts the cellular balance in favor of hyperacetylation, which results in cellular differentiation, apoptosis, and enhanced radiation sensitivity. Thus, the state of chromatin structure is tightly associated with intrinsic cellular radiosensitivity. Our long-term goal of this research is to develop a novel therapeutic strategy by enhancing the radiosensitivity of prostate cancer cells using low concentrations of radiosensitizer and radiation, thereby reducing radiation damage to normal tissue. This will be accomplished by testing **the hypothesis that an increase of cellular radiation sensitivity may be achieved by exposure of cells to certain HDAC inhibitors, leading to a potential clinical translation in the combined modality treatment of prostate cancer.**

BODY

During the first year of the research funding, as outlined in Task I of the statement of work (S.O.W.), we proposed to identify HDAC inhibitors and their effective dose levels for use in the radiation sensitization of prostate cancer cells. The experimental plan includes: (a) Evaluation of the cellular toxicity of HDAC inhibitors in prostate cancer cells. The compounds include TSA, Depsipeptide, SAHA and others if available. (b) Assess acetylation of key proteins associated with inhibitory function of HDAC activity. Some of these factors include histones and non-histone proteins, including those involved in cell cycle regulation. (c) Determination of effects of HDAC inhibitors on cellular radiosensitivity.

The major accomplishments associated with Task I outlined in the S.O.W. include: (1) determination of the values of 50% HDAC inhibition activities of newly synthesized HDAC inhibitors and their anti-proliferation activities in prostate cancer cells. (2) Determination of efficacy of the candidate HDAC inhibitors on cellular radiation sensitivity.

HDAC Inhibition Activities and Cellular Cytotoxicity of HDAC Inhibitors

Newly synthesized biarylalanine analogues of candidate HDAC inhibitors (SW55 and its derivatives, ST groups, as shown in Table 1) were provided by the collaborator (Dr. Manfred Jung). To assess if these compounds possess HDAC inhibitory activities, we first determined the values of the compounds at 50% HDAC inhibition activities and effects on histone acetylation. The data demonstrated that these compounds exhibited the IC_{50} HDAC inhibition values at nanomolar concentrations and enhanced the acetylation level of histone H3/H4 (data not shown). The cytotoxicity levels (IC_{50} values) of these HDAC inhibitors were then determined by performing cell proliferation assays in PC3 cells. The data revealed the IC_{50} anti-proliferation values in a range of 1-50 μ M (Table 1). Although a differential effect was observed with TSA showing greater cytotoxicity than the others in PC3 cells, interestingly, the compound, ST12, conferred as potent as TSA on 50% HDAC inhibitory activity at 30 nM, suggesting that this compound may be a good candidate for our proposed studies. Taken together, HDAC activity inhibition was

dose-dependent, and the 50% HDAC activity inhibition was achieved at nano-molar concentrations of these compounds (Table 1). Although SAHA and depsipeptide were proposed to test in this proposal, we are no longer able to access to these compounds due to intellectual proprietary. Therefore, our proposed studies will utilize these newly designed and synthesized HDAC inhibitors, which do not modify a scope of our proposed studies.

Effects of the compounds on cellular radiation sensitivities

To test the ability of HDAC inhibitors to sensitize cells to radiation, effects of the compounds on cellular radiosensitivity were evaluated by performing clonogenic survival assays. Cells were treated with the compounds at IC₅₀ for 24 h and followed by graded doses of ionizing radiation. Surviving colonies were determined and fit to the single hit multiple-target and the linear quadratic models. In Table 1, radiosensitivity of PC3 cells with HDAC inhibitors, TSA and SAHA, was compared to parental cells (D₀=1.5 Gy). The values of D₀ were significantly decreased in the combined treatment experiments (showing radiation sensitization) comparing radiation with drugs as compared to radiation alone. D₀ values decreased in ranges of 1.10Gy by TSA and 1.32 Gy by SAHA compared with D₀=1.49 Gy of the control with no treatment. SAHA showed modest radiation sensitization as compared to TSA, which efficiently sensitized PC-3 cells.

Taken together, these results suggest that the HDAC inhibitory compounds are effectively sensitize PC3 cells to radiation. It is of particular interest that there is a disparity in radiation sensitizing effectiveness between these compounds. Therefore, we will continue to test effects of SW55 and its derivatives on radiation sensitivity.

Table 1. Effects of HDAC inhibitors in PC cells (D₀=1.49 Gy)

Compound	50% HDAC inhibition activity	Cytotoxicity (IC ₅₀)	Radiation Sensitivity (Gy)
TSA	10 nM	0.3 μ M	1.10 Gy
SAHA	170 nM	1 μ M	1.32 Gy
SW55	290 nM	1 μ M	ND
ST12	30 nM	1.8 μ M	ND
ST16	100 nM	9.9 μ M	ND
ST17	150 nM	50 μ M	ND
ST27	100 nM	10 μ M	ND
ST29	150 nM	10 μ M	ND

ND represents that the experiments are currently in progress.

In addition, we discovered the new role of HDAC7 in prostate cancer epithelial cells. The findings have been reported in detail in JBC (Attached in Appendix).

KEY RESEARCH ACCOMPLISHMENTS:

1. Determination of cytotoxicity profiles of newly synthesized candidate HDAC inhibitors in PC3 cells.
2. Determination of the radiosensitizing effect of a number of HDAC inhibitors.
3. Discovery of a new role of HDAC7: Cytoplasmic sequestration of HDAC7 from mitochondria and nuclear compartment upon initiation of apoptosis.

REPORTABLE OUTCOMES

1. A manuscript published in **JBC279**: 51218-51225, 2004.
2. The second manuscript in preparation.

CONCLUSIONS

During the first year of the research funding, we evaluated cytotoxicity and radiosensitizing property of HDAC inhibitors in PC cells. As shown in Table 1, HDAC activity inhibition was dose-dependent and 50% HDAC inhibition was achieved at nanomolar concentrations of these compounds. Studies of radiosensitization of HDAC inhibitors suggest that the HDAC inhibitory compounds are effectively sensitized PC3 cells to radiation and that there is a disparity in radiation sensitizing effectiveness between these compounds. Testing effects of SW55 and its derivatives on radiation sensitivity is currently in progress. Although SAHA and depsipeptide were proposed to test in this proposal, we are no longer able to access to these compounds due to intellectual proprietary. Therefore, our proposed studies will utilize these newly designed and synthesized HDAC inhibitors, which do not modify a scope of our proposed studies.

REFERENCES: N/A

APPENDICES:

1. Manuscript: Bakin R and Jung M. Cytoplasmic sequestration of HDAC7 from mitochondria and nuclear compartment upon initiation of apoptosis. **JBC279**: 51218-51225, 2004.

Cytoplasmic Sequestration of HDAC7 from Mitochondrial and Nuclear Compartments upon Initiation of Apoptosis*

Received for publication, August 12, 2004, and in revised form, September 1, 2004
Published, JBC Papers in Press, September 9, 2004, DOI 10.1074/jbc.M409271200

Robert E. Bakin and Mira O. Jung†

From the Division of Radiation Research, Department of Radiation Medicine, Lombardi Comprehensive Cancer Center, Georgetown University School of Medicine, Washington, D. C. 20007

Control of global histone acetylation status is largely governed by the opposing enzymatic activities of histone acetyltransferases and deacetylases (HDACs). HDACs were originally identified as modulators of nuclear histone acetylation status and have been linked to chromosomal condensation and subsequent gene repression. Accumulating evidence highlights HDAC modification of non-histone targets. Mitochondria were first characterized as intracellular organelles responsible for energy production through the coupling of oxidative phosphorylation to respiration. More recently, mitochondria have been implicated in programmed cell death whereby release of pro-apoptotic inner membrane space factors facilitates apoptotic progression. Here we describe the novel discovery that the nuclear encoded Class II human histone deacetylase HDAC7 localizes to the mitochondrial inner membrane space of prostate epithelial cells and exhibits cytoplasmic relocation in response to initiation of the apoptotic cascade. These results highlight a previously unrecognized link between HDACs, mitochondria, and programmed cell death.

Originally identified as negative regulators of nuclear histone acetylation, HDACs¹ have been intimately linked to chromatin condensation and subsequent gene repression (1). More recently, increasing evidence has demonstrated HDAC modification of non-histone substrates (2–4) and an involvement in a broader array of biological events including apoptosis (5–8) and radiation sensitivity (9). Human Class I HDACs are generally nuclear proteins homologous to the yeast protein Rpd3 (HDAC1, -2, -3, and -8). Class II HDACs (HDAC4, -5, -6, -7, and -9) are related to HDAC1 and often demonstrate regulated nucleocytoplasmic flux. Class III HDACs are structurally and phylogenetically distinct, being most similar to the NAD⁺-dependent yeast SIR2 proteins.

* This work was supported in part by United States Army Medical Research and Materiel Command Grants PC030471 (to M. O. J.) and PC030019 (to R. E. B.) as well as by the Lombardi Cancer Center Microscopy and Imaging Shared Resource and United States Public Health Service Grants 2P30-CA-51008 and 1S10RR15768-01. The costs of publication of this article were defrayed in part by the payment of page charges. This article must therefore be hereby marked "advertisement" in accordance with 18 U.S.C. Section 1734 solely to indicate this fact.

† To whom correspondence should be addressed: Dept. of Radiation Medicine, The Research Bldg., Rm. E-211, Georgetown University School of Medicine, Box 571482, 3970 Reservoir Rd., N.W., Washington, D. C. 20057-1482. Tel.: 202-687-8352; Fax: 202-687-7529; E-mail: jungm@georgetown.edu.

¹ The abbreviations used are: HDAC, histone deacetylase; IMS, inner membrane space; GFP, green fluorescent protein; FBS, fetal bovine serum; Tricine, N-[2-hydroxy-1,1-bis(hydroxymethyl)ethyl]glycine; AIF, apoptosis-inducing factor; PARP, poly(ADP-ribose) polymerase; NLS, nuclear localization sequence.

HDAC7 is a nuclear encoded Class II HDAC having a conserved C-terminal catalytic domain and a large, highly divergent N-terminal domain implicated in muscle differentiation (10). Cytoplasmic sequestration of HDAC7 can be enhanced by 14-3-3 protein interactions (11) and observed during T cell receptor-mediated apoptosis (8).

Mitochondria were first characterized as intracellular organelles responsible for energy production through the coupling of oxidative phosphorylation to respiration. More recently, mitochondria have been implicated in genetically programmed cell death (12) whereby release of pro-apoptotic mitochondrial inner membrane space factors (13) facilitates the progression of the apoptotic cascade. Dysregulation of the mitochondrial apoptotic program has been linked to both enhanced cell death (14) as well as hyperproliferative growth (15).

Here we describe the novel discovery that the nuclear encoded Class II human histone deacetylase HDAC7 localizes to the mitochondrial inner membrane space (IMS) of several human cell lines, in particular, prostate cancer epithelial cells. Upon induction of the apoptotic cascade, HDAC7 is released from mitochondria and, along with nuclear HDAC7, is redistributed to the cytoplasm. These results highlight a previously unrecognized link between mitochondria, histone deacetylases, and the initiation of apoptosis.

EXPERIMENTAL PROCEDURES

Antibodies and Reagents—Mitochondrial lysate (M22430), ProLong® antifade reagent (P7481), and anti-oxidative complex V (3D5) were purchased from Molecular Probes. Antibodies to HDAC7 (H-273), Tom20 (F-10), AIF (E-1), cytochrome c (6H2), and Smac/DIABLO (C-20) were purchased from Santa Cruz Biotechnology. GFP-Bax was a kind gift from Dr. Tomas Vornastek, University of Virginia. HDAC7-FLAG was a kind gift from Dr. Eric Verdin, UCSF. C4-2 cells were originally obtained from the laboratory of Dr. Leyland Chung, University of Texas Southwestern. Other cell lines were obtained from laboratory frozen stocks and maintained as follows: MRC5CV1 (15% FBS in RPMI, 2 mM L-glutamine, penicillin/streptomycin, 1 mM sodium pyruvate, non-essential amino acids), AT5BIVA (20% FBS, penicillin/streptomycin, 2 mM L-glutamine, non-essential amino acids, 0.1% hydrocortisone), PC-3 (RPMI 1640, 10% FBS), and SQ20B (20% FBS, penicillin/streptomycin, 2 mM L-glutamine, non-essential amino acids, 0.1% hydrocortisone).

Site-directed Mutagenesis—HDAC7-R8P site-directed mutagenesis was carried out using Stratagene QuikChange II XL site-directed mutagenesis kit according to the manufacturer's protocol using the following PAGE-purified primers: forward primer, 5'-GGTGGGCCAG-CCGCCCCAGTGG-3'; and reverse primer, 5'-CCACTGGGGGCGGC-TGGCCCCACC-3'. PCR cycling parameters were as follows: denaturing at 95° C for 50 s, annealing at 60° C for 50 s, and extension for 9 min at 68° C.

Confocal and Non-confocal Immunofluorescent Microscopy—Confocal microscopy was carried out using an Olympus BX61 laser scanning confocal microscope using ×60 oil immersion objective with standard lasers and filter sets for fluorescein isothiocyanate and Texas Red analysis. 4',6-diamidino-2-phenylindole (Sigma) staining was used for non-confocal identification of nucleic acid content. Subsequent confocal image acquisition and analysis were carried out using the Fluoview™

software package. Routine non-confocal indirect immunofluorescence was performed on a Nikon E600 microscope according to standard protocols using fluorescein isothiocyanate and Texas Red secondary antibodies (Jackson Immunologicals) and appropriate optical filter sets. Non-confocal image acquisition and analysis was performed using MetaVue™ (version 5.0.3) imaging analysis software (Universal Imaging Corp.).

Computer Amino Acid Analysis—TopPredII and Kyte-Doolittle hydrophobicity plotting and mitochondrial targeting peptide prediction were performed online.²

Cell Transfections—Routine Lipofectin (Invitrogen) transfection of GFP-Bax was performed according to the manufacturer's protocols. GFP-HDAC7 stable C4-2 cells were selected for G418 and pooled as mass populations.

Western Blotting—Protein samples were run on 10–20% gradient SDS-PAGE Tricine minigels (Invitrogen), blotted to nitrocellulose, and blocked in 5% blocking buffer (Bio-Rad). Primary antibodies were added for 1 h at room temperature, washed in 0.1% SDS, Tween. Secondary horseradish peroxidase-conjugated antibodies were added for 1 h at room temperature and washed in 0.1% SDS, Tween. Blots were developed in ECL reagent (Amersham Biosciences) and exposed to film (Amersham Biosciences).

Mitochondria Isolation, Permeabilization, and Subfractionation—Mitochondria were isolated from 80% confluent C4-2 cell monolayers using a Pierce mitochondrial isolation kit according to the manufacturer's instructions with the addition of complete EDTA-free protease inhibitor mixture (Roche Applied Science). For permeabilization of the mitochondrial outer membrane (16), cells were plated on glass coverslips for 3 days and then treated with either 0.01 or 0.5% saponin in 4% paraformaldehyde for 30 min at room temperature. Routine indirect immunofluorescence was subsequently carried out using the appropriate primary and secondary fluorescent antibodies.

Mitochondrial subfractionation was carried out on freshly isolated mitochondria. Isolated mitochondria were immediately subfractionated according to protocols established by Greenawalt (17). Briefly, purified mitochondria were resuspended in isolation medium (70 mM sucrose, 220 mM D-mannitol, 2 mM HEPES, 0.5 mg/ml bovine serum albumin adjusted to pH 7.4 with KOH) at a concentration of 100 mg/ml. An equal volume of stock 1.2% digitonin medium was then added and stirred gently on ice for 15 min. Three more volumes of isolation medium were then added and centrifuged at 10,000 × *g* for 10 min. The sediment consisted of the crude mitoplast (*i.e.* inner membrane and matrix components) fraction. The supernatant was removed and centrifuged at 144,000 × *g* for 60 min. Pelleted material contained mitochondrial outer membranes, whereas the remaining fluid consisted largely of soluble inner membrane proteins.

Imaging of Live Cells—All live imaging was carried out using a Nikon TE300 live imaging system with ×60 oil immersion objective using MetaMorph 6.1 software (Universal Imaging Corporation). MitoTracker Red® was added to culture medium for 30 min according to the manufacturer's protocols.

RESULTS

Mitochondrial Localization of Mammalian HDAC7—Nuclear encoded proteins destined for mitochondria contain cleavable N-terminal signaling peptides of degenerate amino acid length and composition that are necessarily removed after mitochondrial import (18, 19). N-terminal primary amino acid analysis of human HDAC7 identified a novel mitochondrial targeting presequence (20) in both mammalian isoforms of HDAC7 that was not present in any other known human HDAC (Fig. 1A). This presequence was moderately conserved in both rat and mouse, albeit with divergent N-terminal amino acid additions of unknown biological significance. Mitochondrial targeting presequences often exhibit a conserved amphipathic α -helix containing clustered positively charged hydrophobic and hydroxylated amino acid residues (21). HDAC7 secondary structure analysis of the N terminus revealed a clustering of basic amino acids commonly observed in amphipathic α -helical structures, including the NAD⁺-dependent and mitochondrial localized human Class III deacetylase SIRT3 (Fig. 1B).

Confocal laser microscopy of untreated human prostate epithelial C4-2 cells revealed robust and distinct colocalization of endogenous HDAC7 with the mitochondria-specific proteins Hsp60, Tom20, and AIF (Fig. 2A). Similar mitochondria-specific localization of HDAC7 was observed in other human cell lines including AT5BIVA and MR5CV1 fibroblasts as well as PC-3 epithelial cells (Fig. 2B), suggesting that mitochondrial HDAC7 localization may be a general biological phenomenon of human cells. Live imaging of stable expression of N-terminal GFP-tagged HDAC7 (GFP-HDAC7) similarly exhibited colocalization with the mitochondria-specific dye MitoTracker Red (Fig. 2C).

HDAC7 Is N-terminally Processed in Mitochondria—By an incompletely understood mechanism, three peptidases mediate a physiologically necessary endoproteolytic cleavage of both nuclear and mitochondria-encoded precursor polypeptides destined for mitochondrial residence (22, 23). Failure to remove such targeting presequences has been implicated in human disease including the pathophysiology of Friedreich ataxia (24, 25). Mitochondrial processing peptidase initially cleaves the vast majority of N-terminal mitochondrial targeting presequences. Based on additional uncharacterized protein targeting motifs downstream of the mitochondria-processing peptidase site, inner membrane peptidase and mitochondrial intermediate peptidase subsequently process specific subsets of precursor polypeptides destined for various mitochondrial subcompartments.

Amino acid sequencing predicts an approximate molecular mass of around 100 and 96 kDa for HDAC7a and HDAC7b, respectively. Analysis of HDAC7 protein expression in C4-2 cells consistently failed to identify an HDAC7 species of this size. Suggesting that the majority of HDAC7 in C4-2 cells is proteolytically processed in mitochondria, we routinely observe a truncated form of HDAC7 (~80 kDa) in both C4-2 mitochondrial preparations as well as commercially available heart mitochondrial protein lysates (Fig. 3A).

Current mitochondrial presequence processing site motifs are ill defined, thus precluding site-directed mutagenesis analysis. As mitochondrial import of HDAC7 is a prerequisite for N-terminal proteolytic processing of HDAC7, we reasoned that mutation of structurally important basic amino acid residues in the N-terminal presequence α -helix would attenuate mitochondrial import and thus prevent processing of full-length HDAC7. Transient overexpression of C-terminal FLAG-tagged HDAC7 containing the R8P mutation (HDAC7-R8P) in parental C4-2 cells resulted in expression of only unprocessed, full-length HDAC7 (Fig. 3B). As a control, we similarly transfected the HDAC7-R8P mutant into C4-2 cells stably expressing wild type HDAC7-FLAG. Here, both the unprocessed form of HDAC7-R8P (Fig. 3B, upper band) as well as the mitochondrially processed form (Fig. 3B, lower band) of wild type HDAC7 were observed. In sum, we demonstrate that HDAC7 mitochondrial import is dependent upon a structurally intact targeting presequence and that localization of HDAC7 to mitochondria results in proteolytic removal of the targeting presequence.

HDAC7 Is a Mitochondrial Inner Membrane Space Protein—Undefined cryptic secondary targeting peptides within the mitochondrial targeting presequence dictate which subcompartment will eventually receive a protein. Kyte-Doolittle hydrophobicity plotting and TopPred II software analysis (26) both identify HDAC7 as a relatively hydrophilic protein with no significant regions of hydrophobicity commonly associated with membrane proteins (data not shown). Mitochondrial subfractionation of untreated C4-2 mitochondria reveals that HDAC7 colocalizes with known soluble mitochondrial IMS proteins AIF and Smac/DIABLO (Fig. 4A). Tom20 and the oxida-

² R. Bakin and M. Jung, personal communication.

(A)

human (a)	1
human (b)	1
mouse	1
rat	1	MNWWSPLECKPEPPLLEITLLEASIAVVGILLNCGFFLDDGGFFMAVVPVSLKPKQVSVISIGWLLGACFGCPGKMSVSTSGR
human (a)	1
human (b)	1
mouse	1
rat	81	REGTAGHTFTSLSTDGTRVSLGACCPWFPGTGCVLSRGDEQQQTRAQPIELILGLLPPLDSYGAVSSQRGVQEEGPPPTL
human (a)	1
human (b)	1
mouse	1
rat	161	KQPHLPASQHPWPLSLAAGYAGTAPGLPDTPGQGPMDLVGOVGOVPPVEPPPEPTLLALOPDILLLFLLAGLQQQ
human (a)	42	SVEPMKLSMDTPMPELOVGPQEQELQLLHKDKSKSAVASVSVKQKLAEVILKKQQAALERTVHPNSPGIPYRTLEPLE
human (b)	42	SVEPMKLSMDTPMPELOVGPQEQELQLLHKDKSKSAVASVSVKQKLAEVILKKQQAALERTVHPNSPGIPYRTLEPLE
mouse	65	SAEPMKLSMDTPMPELOVGPQEQELQLLHKDKSKSAVASVSVKQKLAEVILKKQQAALERTVHPNSPGIPYRTLEPLE
rat	241	SAEPMKLSMDTPMPELOVGPQEQELQLLHKDKSKSAVASVSVKQKLAEVILKKQQAALERTVHPNSPGIPYRTLEPLE
human (a)	122	TEGATRSMLSSFLPPVPSPSPDPPEHFPPLRKTVSEPNLKLRYKPKKSLERRKNPILRRKESAPPSLRRRPAAETLGDSSPSS
human (b)	122	TEGATRSMLSSFLPPVPSPSPDPPEHFPPLRKTVSEPNLKLRYKPKKSLERRKNPILRRKESAPPSLRRRPAAETLGDSSPSS
mouse	145	TEGATRSMLSSFLPPVPSPSPDPPEHFPPLRKTVSEPNLKLRYKPKKSLERRKNPILRRKESAPPSLRRRPAAETLGDSSPSS
rat	321	TEGATRSMLSSFLPPVPSPSPDPPEHFPPLRKTVSEPNLKLRYKPKKSLERRKNPILRRKESAPPSLRRRPAAETLGDSSPSS
human (a)	202	SSTPASGCSNDSSEHGPNPILGSEALLGQRLRLQETSVPAPFALPTVSLPAITLGLPAPARADSDRRHTPTLGPGRGPIIL
human (b)	202	SSTPASGCSNDSSEHGPNPILGSEALLGQRLRLQETSVPAPFALPTVSLPAITLGLPAPARADSDRRHTPTLGPGRGPIIL
mouse	225	SSTPASGCSNDSSEHGPNPILGSEALLGQRLRLQETSVPAPFALPTVSLPAITLGLPAPARADSDRRHTPTLGPGRGPIIL
rat	401	SSTPASGCSNDSSEHGPNPILGSEALLGQRLRLQETSVPAPFALPTVSLPAITLGLPAPARADSDRRHTPTLGPGRGPIIL
human (a)	282	GSPHPLFLFLPHGLEPEAGGTLPSRLQPIILLLOPSGSHAPILLTPVGLGDLPPHFAQSLMTTERLCSGSLHWPILSRTSRSEPL
human (b)	282	GSPHPLFLFLPHGLEPEAGGTLPSRLQPIILLLOPSGSHAPILLTPVGLGDLPPHFAQSLMTTERLCSGSLHWPILSRTSRSEPL
mouse	268	GSPHPLFLFLPHGLEPEAGGTLPSRLQPIILLLOPSGSHAPILLTPVGLGDLPPHFAQSLMTTERLCSGSLHWPILSRTSRSEPL
rat	481	GSPHPLFLFLPHGLEPEAGGTLPSRLQPIILLLOPSGSHAPILLTPVGLGDLPPHFAQSLMTTERLCSGSLHWPILSRTSRSEPL
human (a)	362	PPSATAPPPPPPMQPRILEQLKTHVQVVK.....RSAKPSSEKPRRLQIPSAEDLETDCGGGPGQVVDGGLHRELGNGGDP
human (b)	322	PPSATAPPPPPPMQPRILEQLKTHVQVVK.....RSAKPSSEKPRRLQIPSAEDLETDCGGGPGQVVDGGLHRELGNGGDP
mouse	348	PPSATAPPPPPPMQPRILEQLKTHVQVVK.....RSAKPSSEKPRRLQIPSAEDLETDCGGGPGQVVDGGLHRELGNGGDP
rat	561	PPSATAPPPPPPMQPRILEQLKTHVQVVK.....RSAKPSSEKPRRLQIPSAEDLETDCGGGPGQVVDGGLHRELGNGGDP
human (a)	435	EARGCAPLQOHPQVLLWEQOHLAAGRLPRLPGSTGOTVLLPLAQGGHRRPLSRAQSSPAAPASLSAPEPASOARVLSSETPAR
human (b)	395	EARGCAPLQOHPQVLLWEQOHLAAGRLPRLPGSTGOTVLLPLAQGGHRRPLSRAQSSPAAPASLSAPEPASOARVLSSETPAR
mouse	428	EARGCAPLQOHPQVLLWEQOHLAAGRLPRLPGSTGOTVLLPLAQGGHRRPLSRAQSSPAAPASLSAPEPASOARVLSSETPAR
rat	641	EARGCAPLQOHPQVLLWEQOHLAAGRLPRLPGSTGOTVLLPLAQGGHRRPLSRAQSSPAAPASLSAPEPASOARVLSSETPAR
human (a)	515	TLPTFTGLIYDSVMLKHQCSGCGNSRHPHAGRIOSIWSRLQERGLRSQCECLRGRKASLEELQSVHSEHNVLLVYCTNPL
human (b)	475	TLPTFTGLIYDSVMLKHQCSGCGNSRHPHAGRIOSIWSRLQERGLRSQCECLRGRKASLEELQSVHSEHNVLLVYCTNPL
mouse	507	TLPTFTGLIYDSVMLKHQCSGCGNSRHPHAGRIOSIWSRLQERGLRSQCECLRGRKASLEELQSVHSEHNVLLVYCTNPL
rat	720	TLPTFTGLIYDSVMLKHQCSGCGNSRHPHAGRIOSIWSRLQERGLRSQCECLRGRKASLEELQSVHSEHNVLLVYCTNPL
human (a)	595	SRKLKLDNGKLAGLLAQRMFVMLPCGGGVGDVDTIWNELHSNAARWAAGSVTDLAFKVASRELK.....NGFAVVRP
human (b)	555	SRKLKLDNGKLAGLLAQRMFVMLPCGGGVGDVDTIWNELHSNAARWAAGSVTDLAFKVASRELK.....NGFAVVRP
mouse	582	SRKLKLDNGKLAGLLAQRMFVMLPCGGGVGDVDTIWNELHSNAARWAAGSVTDLAFKVASRELK.....NGFAVVRP
rat	795	SRKLKLDNGKLAGLLAQRMFVMLPCGGGVGDVDTIWNELHSNAARWAAGSVTDLAFKVASRELK.....NGFAVVRP
human (a)	667	PGHHAHDSHTAMGFCFFNSVAIACRQLQOQSKASKILLVDWDVHHNGTQQTIFYQDPSVLYISLHRHDDGNFFPGSGAVDE
human (b)	627	PGHHAHDSHTAMGFCFFNSVAIACRQLQOQSKASKILLVDWDVHHNGTQQTIFYQDPSVLYISLHRHDDGNFFPGSGAVDE
mouse	654	PGHHAHDSHTAMGFCFFNSVAIACRQLQOQSKASKILLVDWDVHHNGTQQTIFYQDPSVLYISLHRHDDGNFFPGSGAVDE
rat	675	PGHHAHDSHTAMGFCFFNSVAIACRQLQOQSKASKILLVDWDVHHNGTQQTIFYQDPSVLYISLHRHDDGNFFPGSGAVDE
human (a)	747	VGAGSGEGFNHNVAVAGGLDPPMGDPEYLAFAFRIVVMPIAREFSPDLVLSAGFDAAEGHPAPLGGYHVSAKCFGYMTQQ
human (b)	707	VGAGSGEGFNHNVAVAGGLDPPMGDPEYLAFAFRIVVMPIAREFSPDLVLSAGFDAAEGHPAPLGGYHVSAKCFGYMTQQ
mouse	734	VGAGSGEGFNHNVAVAGGLDPPMGDPEYLAFAFRIVVMPIAREFSPDLVLSAGFDAAEGHPAPLGGYHVSAKCFGYMTQQ
rat	955	VGAGSGEGFNHNVAVAGGLDPPMGDPEYLAFAFRIVVMPIAREFSPDLVLSAGFDAAEGHPAPLGGYHVSAKCFGYMTQQ
human (a)	827	LMNLAGGAVVLALEGGHDLTAICDASEACVAAILGNRVDPISSEEGWKQKPNLNAIRSLAVIRVHSKY.....
human (b)	787	LMNLAGGAVVLALEGGHDLTAICDASEACVAAILGNRVDPISSEEGWKQKPNLNAIRSLAVIRVHSKY.....
mouse	814	LMNLAGGAVVLALEGGHDLTAICDASEACVAAILGNRVDPISSEEGWKQKPNLNAIRSLAVIRVHSKY.....
rat	1035	LMNLAGGAVVLALEGGHDLTAICDASEACVAAILGNRVDPISSEEGWKQKPNLNAIRSLAVIRVHSKY.....
human (a)	895WGCMQRLASCPDSWVPRVPGADKEEVEAVTALASLSVGILAEOR
human (b)	855WGCMQRLASCPDSWVPRVPGADKEEVEAVTALASLSVGILAEOR
mouse	882WGCMQRLASCPDSWVPRVPGADKEEVEAVTALASLSVGILAEOR
rat	1115	NHEEDIRGLVGEPOREPQIELTVEPLVGLLVIGKYWGCMQRLASCPDWLPRVPGADAEVEAVTALASLSVGILAEOR
human (a)	999	PSEQLVEEEEPNNL
human (b)	999	PSEQLVEEEEPNNL
mouse	925	PSEQLVEEEEPNNL
rat	1193	PSEQLVEEEEPNNL

(B)

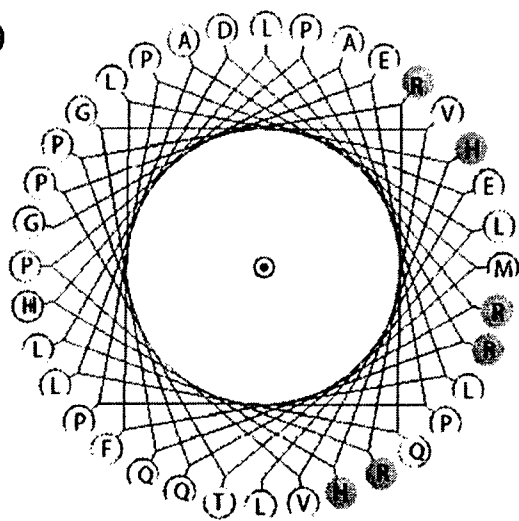


FIG. 1. Human HDAC7 contains a mitochondrial targeting presequence. A, **bold underline** approximates region of mitochondrial targeting presequence, and **dashed underline** approximates mitochondrial inner membrane space secondary targeting sequence. Gray vertical rectangles identify structurally important basic residues. Large rectangle identifies region of positively charged NLS. Small rectangle denotes nuclear export sequence. B, helical wheel plot of HDAC7 N terminus. Clustered positively charged residues are highlighted.

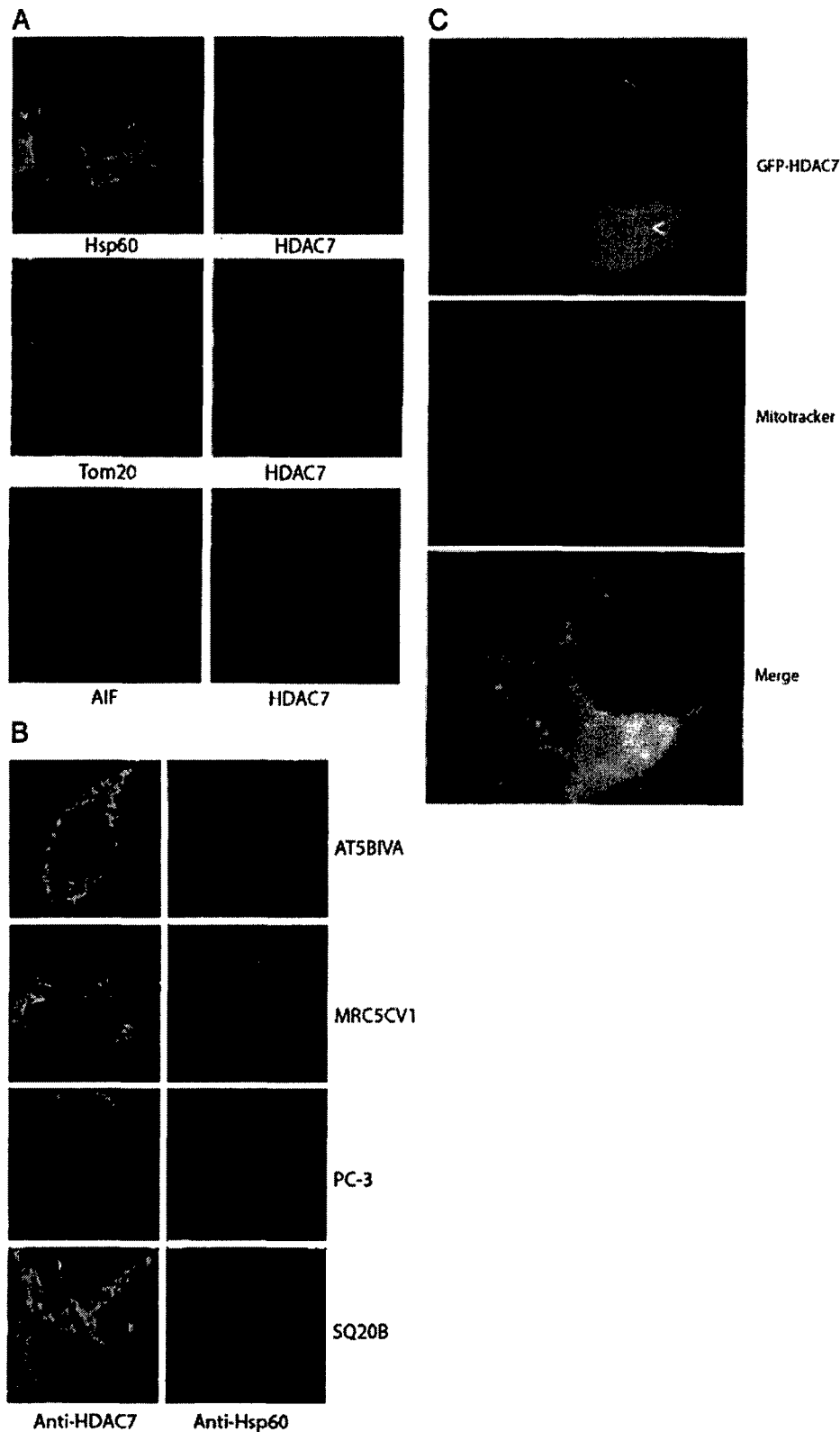


FIG. 2. HDAC7 colocalizes with mitochondria-specific proteins. *A*, confocal microscopy colocalizes endogenous human HDAC7 with the mitochondria-specific proteins Hsp60, Tom20, and AIF in untreated C4-2 prostate cancer cells. *B*, HDAC7 localizes to the mitochondria of AT5BIVA, MRC5CV1, PC-3, and SQ20B human cell lines. *C*, stable expression N-terminal GFP-HDAC7 colocalizes with the mitochondrial marker MitoTracker Red.

tive phosphorylation complex V served as controls for the outer membrane and inner membrane/matrix (*e.g.* mitoplasts) compartments of mitochondria, respectively.

If HDAC7 is a soluble mitochondrial IMS protein, permeabilization of the mitochondrial outer membrane should result in release of HDAC7. Mitochondrial outer membranes were selec-

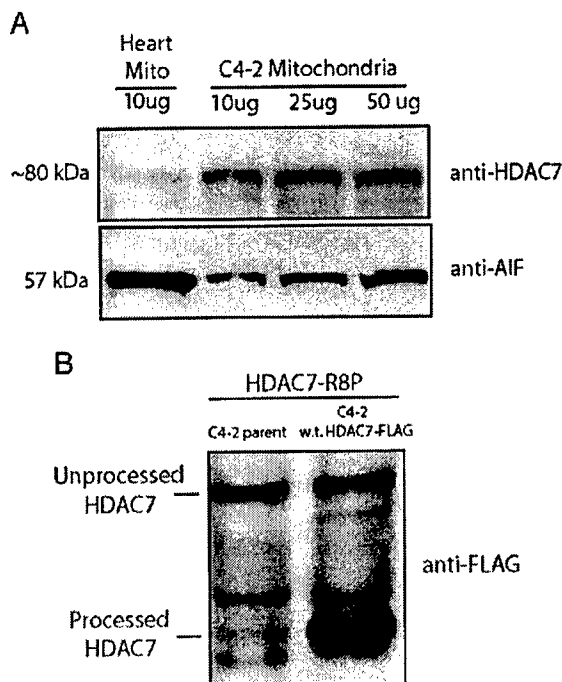


FIG. 3. HDAC7 is N-terminally processed in mitochondria. *A*, Western blot analysis of commercially isolated heart mitochondria (Mito) and C4-2 prostate cell mitochondrial preparations identifies an ~80-kDa truncated HDAC7 species. *B*, mutation of structurally important positively charged residues (R8P) in the mitochondrial targeting presequence results in a failure to process HDAC7. Parental C4-2 cells and C4-2 cells stably expressing wild type (*w.t.*) HDAC7-FLAG were transiently transfected with HDAC7-R8P and Western blotted for FLAG epitope.

tively permeabilized with either the mild detergent saponin (16) or transient overexpression of the pro-apoptotic protein Bax (27). Bax recruitment to mitochondria has been shown to trigger mitochondrial outer membrane permeabilization resulting in the release of pro-apoptotic IMS proteins. Saponin membrane permeabilization resulted in a substantial loss of canonical mitochondrial HDAC7 staining and default relocalization of HDAC7 to punctate nuclear bodies that intensified with increased detergent concentration (Fig. 4*B*). Finally, GFP-Bax overexpression promoted mitochondrial release of AIF, cytochrome *c*, and HDAC7 in addition to nuclear DNA fragmentation (Fig. 4*C*). In sum, we demonstrate that HDAC7 is a soluble mitochondrial IMS protein the retention of which is dependent upon an intact mitochondrial outer membrane. Moreover, HDAC7 mitochondrial release closely parallels the translocation dynamics of several recognized IMS proteins implicated in programmed cell death.

Cytoplasmic Sequestration of HDAC7 under Pro-apoptotic Conditions—Seminal studies of HDAC7 have demonstrated regulated nucleocytoplasmic shuttling resulting in the differentiation of myocytes (11). Cytoplasmic relocalization of HDAC7 has additionally been implicated in thymocyte cell death (8). In light of these reports and our demonstration that HDAC7 can localize to multiple subcellular compartments, including the mitochondrial IMS, we further characterized the translocation dynamics of HDAC7 under pro-apoptotic conditions.

Although still competent for apoptosis as evidenced by GFP-Bax transient overexpression, a variety of known apoptosis agents including Fas-L, LY294002, forskolin, serum starvation, ionizing radiation, and cisplatin failed to readily induce mass apoptosis in these cells as measured by PARP and Bid cleavage as well as H2A.X phosphorylation (data not shown).

We demonstrate that a reliable initiator of the apoptotic cascade in C4-2 cells was the aminoglycoside and protein translation inhibitor hygromycin. 48-hour treatment with 100 μ g/ml hygromycin readily and reproducibly induced both PARP and Bid cleavage as well as phosphorylation of H2A.X (Fig. 5*a*).

We next treated C4-2 cells with 100 μ g/ml hygromycin for 48 h and fractionated cells into cytoplasmic, mitochondrial, and nuclear components. Results demonstrate a near complete redistribution of HDAC7 from mitochondrial to cytoplasmic pools (Fig. 5*b*). Finally, we demonstrate via live cell imaging of hygromycin-treated C4-2 cells stably expressing GFP-HDAC7 a near complete redistribution of GFP-HDAC7 in the cytoplasm after 9 h (Fig. 6). This was most dramatic in the low percentage of cells where GFP-HDAC7 initially was localized to the nucleus. Cytoplasmic HDAC7 sequestration remained unchanged for the remainder of the 48-h experiment (data not shown).

Here we report the localization of a Class II HDAC to the mitochondrial IMS of normally growing human prostate epithelial cells. Similar to other nuclear encoded mitochondrial proteins, we demonstrate that mitochondrial import of HDAC7 results in N-terminal truncation and residence in the inner membrane space. Similar to other pro-apoptotic mitochondrial IMS proteins, HDAC7 is released from mitochondria into the cytoplasm upon onset of programmed cell death where it is sequestered exclusively in the cytoplasm.

DISCUSSION

Here we describe the novel finding of a human Class II HDAC localized to the mitochondrial inner membrane space of human prostate cancer cells. As we observe similar localization of HDAC7 in other human cell lines including AT5BIVA and MR5CV1 fibroblasts as well as PC-3 and LNCaP (data not shown) prostate cancer cells, we propose that such a phenomenon is likely not the exception to the rule. Similar to other mitochondrial nuclear encoded proteins, HDAC7 contains a targeting presequence that is necessarily proteolyzed by mitochondrial enzymes by an incompletely understood mechanism. Suggestively, HDAC7 is sequestered in a mitochondrial compartment shown previously to contain several pro-apoptotic proteins and displays translocation dynamics in response to apoptotic stimuli similar to those of other reported pro-apoptotic factors such as cytochrome *c* and Smac/DIABLO. As apoptosis is an evolutionarily well conserved mechanism, it would not be surprising to find HDAC7 in the mitochondria of other human cell types.

A recent report implicates HDAC7 in thymocyte apoptosis (5). Here, HDAC7 nuclear export during T cell receptor activation derepresses expression of the orphan transcription factor Nur77 leading to apoptosis. Highlighting a potential pro-apoptotic role of cytoplasmic (or at least non-nuclear) HDAC7, it was further demonstrated that a triple HDAC7 mutant unable to exit the nucleus (and thus unable to enter the cytoplasm) suppressed T cell receptor-mediated apoptosis (5). HDAC7 has been shown to inhibit the expression of Nur77 via the transcription factor MEF2D. Interestingly, the MEF2D binding domain lies in the same N-terminal region of HDAC7 that contains the mitochondrial targeting presequence.

Mitochondrial targeting presequences normally consist of a positively charged motif of 20–60 residues, often followed by vaguely defined intramitochondrial sorting peptides. Although not the focus of this study, it seems reasonable to conclude that the presequence does not extend into the NLS as HDAC7 demonstrates nuclear localization. Western blotting of stably transfected GFP-HDAC7 C4-2 cells for GFP detects an ~35-kDa band (data not shown). GFP is a 27-kDa protein suggesting that the additional 8 kDa (~70 amino acids) originates from the mitochondrial targeting presequence of HDAC7. These val-

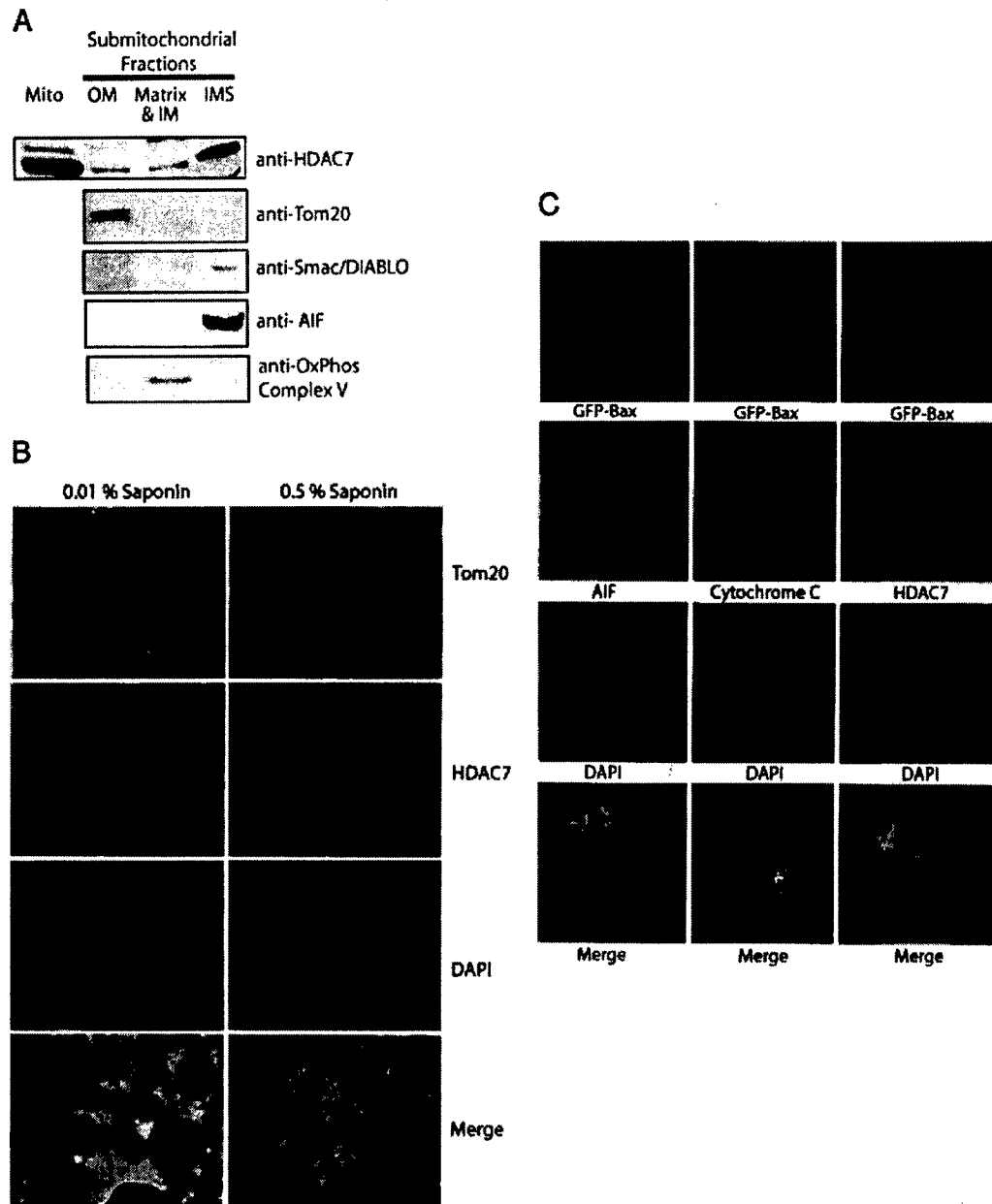


FIG. 4. HDAC7 is a mitochondrial inner membrane space protein. *A*, submitochondrial fractionation localizes HDAC7 to the inner membrane space. *Mito*, mitochondria; *OM*, outer membrane; *IM*, inner membrane; *IMS*, inner membrane space; *OxPhos*, oxidative phosphorylation. *B*, detergent permeabilization of mitochondrial outer membrane results in release of HDAC7 from mitochondria and default nuclear relocalization. *C*, GFP-Bax overexpression results in release of the mitochondrial inner membrane space proteins AIF, cytochrome c, and HDAC7.

ues are entirely compatible with our data. The significance of the N-terminal extensions of mouse and rat HDAC7 is unknown with respect to mitochondrial localization and function. As we routinely observed N-terminally tagged GFP-HDAC7 in the mitochondria of cells, we speculated that N-terminal peptide additions to the targeting presequence may not ultimately affect mitochondrial import. One interesting observation is that whereas we often observed HDAC7 in both the nucleus and cytoplasm of both live and fixed cells, when HDAC7 is localized to mitochondria it is often robust and exclusively mitochondrial. Although the specific cellular condition(s) regulating HDAC7 mitochondrial import are unknown, this observation is likely because of either enhanced HDAC7 mitochondrial import or attenuated release. As 14-3-3 proteins favor cytoplasmic sequestration of phosphorylated HDAC7, and mitochondria are located in the cytoplasm, it is tempting to

speculate that kinase activity might ultimately enhance mitochondrial import. Finally, mitochondrially processed HDAC7 is still technically competent for cytonuclear flux as both the NLS and nuclear export sequence remain intact. Indeed, the NLS is now at a more N-terminal site, introducing the concept that mitochondrial processing might be revealing an otherwise masked NLS. This brings up the interesting possibility that mitochondrial processed HDAC7 might have enhanced nuclear import capabilities relative to full-length, unprocessed HDAC7.

We were initially surprised to identify HDAC7 in mitochondria as previous reports have shown dramatic cytoplasmic and nuclear localization of HDAC7. Curiously, whereas we observed occasional nondescript localization of HDAC7 in both the cytoplasm and nucleus of individual cells (Fig. 6), when we did observe mitochondrial HDAC7 in individual cells it was

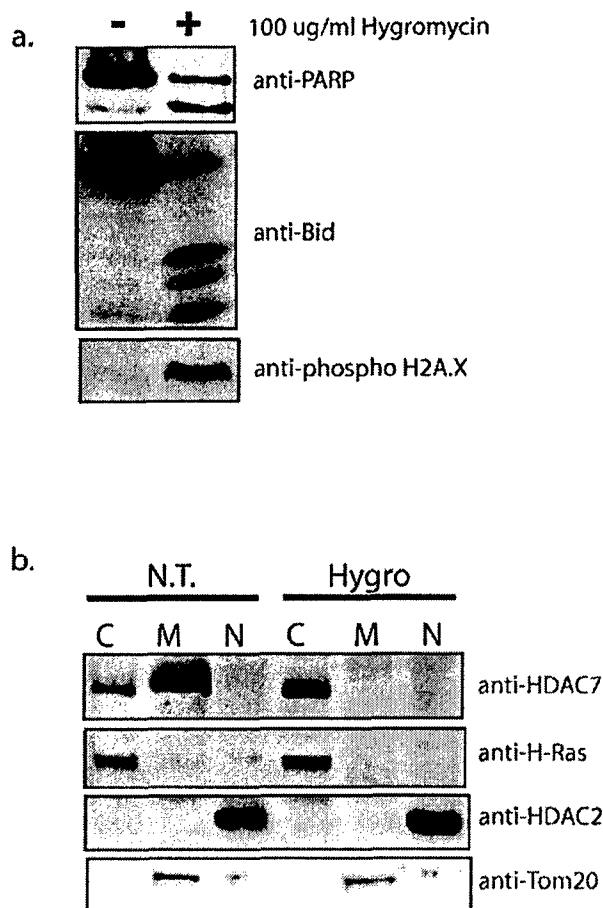


FIG. 5. Initiation of apoptosis results in cytoplasmic sequestration of HDAC7. *a*, hygromycin readily initiates apoptosis in C4-2 cells. 48-h treatment with 100 µg/ml hygromycin induces PARP cleavage, Bid processing, and H2A.X phosphorylation. *b*, hygromycin promotes cytoplasmic sequestration of mitochondrial HDAC7. H-Ras, HDAC2, and Tom20 were used as cytoplasmic, nuclear, and mitochondria-specific markers, respectively. *N.T.*, no treatment; *C*, cytoplasmic; *M*, mitochondrial; *N*, nuclear.

robust and exclusively mitochondrial more often than not. On rare occasions, we observed both punctate mitochondrial localization of GFP-HDAC7 in a background of general cytoplasmic staining (Fig. 2*C*, top image, lower right GFP-positive cell). Integrating our data into current models of HDAC7 cellular localization, we propose that mitochondrial HDAC7 localization can, at least under certain cellular conditions, be obscured by a more intense general cytoplasmic HDAC7 signal. Furthermore, as the GFP tag was N-terminal in our studies and all known mitochondrial imported proteins had their N-terminal targeting peptide removed via endoproteolytic cleavage, we propose that the cytoplasmic and nuclear GFP-HDAC7 that we observed at no time resided in the mitochondrial inner membrane space. Importantly, this species of HDAC7 is competent to enter mitochondria as the targeting presequence would still be intact. In this model, mitochondria could act as an irreversible intracellular reservoir (at least in non-apoptotic cells) to sequester HDAC7 that would otherwise be available for cyto-nuclear flux, and this may offer a novel method of epigenetic regulation of the genome. As mitochondrial HDAC7 likely is involved in different biological events relative to unprocessed, full-length HDAC7, we speculate that the repertoire of interacting proteins might be considerably different from those previously reported for non-mitochondrial HDAC7 (10). As HDAC7 is a regulated phosphoprotein and can exist in either

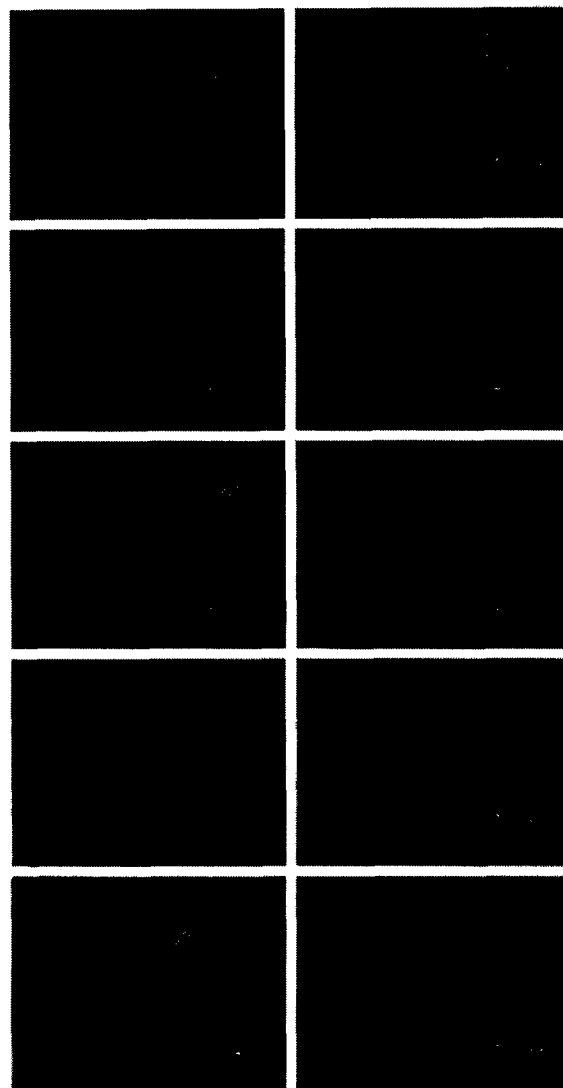


FIG. 6. Apoptotic stimulus results in cytoplasmic accumulation of GFP-HDAC7 in live cells. C4-2 cells stably expressing GFP-HDAC7 were exposed to 100 µg/ml hygromycin for 24 h and imaged every h via time course live imaging.

cytoplasmic, nuclear, or mitochondrial compartments of individual cells or even the same cell, we conclude that the regulation of HDAC7 intracellular localization is likely quite complex. In sum, we have demonstrated the novel finding that HDAC7 can localize to mitochondria in addition to previous reports demonstrating cytoplasmic and nuclear HDAC7 localization.

As mentioned earlier, mitochondrial release of N-terminally processed HDAC7 and subsequent cytoplasmic sequestration might be directly involved in programmed cell death under apoptotic conditions. Although we readily observed PARP and Bid cleavage as well as H2A.X phosphorylation in response to hygromycin treatment, we routinely failed to observe H2B phosphorylation. H2B phosphorylation has recently been proposed as a definitive marker of commitment to apoptosis (28). Although this marker may eventually become apparent at later time points, under the conditions and time points at which we observed HDAC7 translocation to the cytoplasm, commitment to apoptosis might not be assured.

Taken together, as HDAC7 appears to be the only known HDAC localized to mitochondria, we speculate that HDAC7 has

a unique and complex role in normal cellular function, quite possibly apoptosis. Future studies are under way to identify cytoplasmic substrates and further characterize the significance of mitochondrial HDAC7 in the process of programmed cell death.

Acknowledgments—We thank Dr. Tomas Vomastek for the GFP-Bax expression vector and Dr. Eric Verdin for the wild type HDAC7-FLAG expression vector.

REFERENCES

- Strahl, B. D., and Allis, C. D. (2000) *Nature* **403**, 41–45
- North, B. J., Marshall, B. L., Borra, M. T., Denu, J. M., and Verdin, E. (2003) *Mol. Cell* **11**, 437–444
- Luo, J., Nikolaev, A. Y., Imai, S., Chen, D., Su, F., Shiloh, A., Guarente, L., and Gu, W. (2001) *Cell* **107**, 137–148
- Zhang, Y., Li, N., Caron, C., Matthias, G., Hess, D., Khochbin, S., and Matthias, P. (2003) *EMBO J.* **22**, 1168–1179
- Dequiedt, F., Kasler, H., Fischle, W., Kiermer, V., Weinstein, M., Herndier, B. G., and Verdin, E. (2003) *Immunity* **18**, 687–698
- Liu, F., Dowling, M., Yang, X. J., and Kao, G. D. (2004) *J. Biol. Chem.* **279**, 34537–34546
- Paroni, G., Mizzau, M., Henderson, C., Del Sal, G., Schneider, C., and Brancolini, C. (2004) *Mol. Biol. Cell* **15**, 2804–2818
- Verdin, E., Dequiedt, F., and Kasler, H. (2004) *Novartis Found. Symp.* **259**, 115–131, 163–169
- Zhang, Y., Jung, M., and Dritschilo, A. (2004) *Radiat. Res.* **161**, 667–674
- Dressel, U., Bailey, P. J., Wang, S. C., Downes, M., Evans, R. M., and Muscat, G. E. (2001) *J. Biol. Chem.* **276**, 17007–17013
- Kao, H. Y., Verdel, A., Tsai, C. C., Simon, C., Juguilon, H., and Khochbin, S. (2001) *J. Biol. Chem.* **276**, 47496–47507
- Desagher, S., and Martinou, J. C. (2000) *Trends Cell Biol.* **10**, 369–377
- Suzuki, Y., Imai, Y., Nakayama, H., Takahashi, K., Takio, K., and Takahashi, R. (2001) *Mol. Cell* **8**, 613–621
- Jordan, J., Cena, V., and Prehn, J. H. (2003) *J. Physiol. Biochem.* **59**, 129–141
- Hu, W., and Kavanagh, J. J. (2003) *Lancet Oncol.* **4**, 721–729
- Schulz, I. (1990) *Methods Enzymol.* **192**, 280–300
- Greenawalt, J. W. (1974) *Methods Enzymol.* **31**, 310–323
- Rapaport, D. (2003) *EMBO Rep.* **4**, 948–952
- Hartl, F. U., Pfanner, N., Nicholson, D. W., and Neupert, W. (1989) *Biochim. Biophys. Acta* **988**, 1–45
- Emanuelsson, O., Nielsen, H., Brunak, S., and von Heijne, G. (2000) *J. Mol. Biol.* **300**, 1005–1016
- Schwer, B., North, B. J., Frye, R. A., Ott, M., and Verdin, E. (2002) *J. Cell Biol.* **158**, 647–657
- Gakh, O., Cavadini, P., and Isaya, G. (2002) *Biochim. Biophys. Acta* **1592**, 63–77
- Ito, A. (1999) *Biochem. Biophys. Res. Commun.* **265**, 611–616
- Patel, P. I., and Isaya, G. (2001) *Am. J. Hum. Genet.* **69**, 15–24
- Branda, S. S., Cavadini, P., Adamec, J., Kalousek, F., Taroni, F., and Isaya, G. (1999) *J. Biol. Chem.* **274**, 22763–22769
- Claros, M. G., and von Heijne, G. (1994) *Comput. Appl. Biosci.* **10**, 685–686
- Kuwana, T., Mackey, M. R., Perkins, G., Ellisman, M. H., Latterich, M., Schneider, R., Green, D. R., and Newmeyer, D. D. (2002) *Cell* **111**, 331–342
- Cheung, W. L., Ajiro, K., Samejima, K., Kloc, M., Cheung, P., Mizzen, C. A., Beeser, A., Etkin, L. D., Chernoff, J., Earnshaw, W. C., and Allis, C. D. (2003) *Cell* **113**, 507–517